ChemComm

COMMUNICATION

View Article Online
View Journal

Cite this: DOI: 10.1039/d6cc01304j

Received 5th March 2026,
Accepted 17th April 2026

DOI: 10.1039/d6cc01304j

rsc.li/chemcomm

Unified, catalyst-controlled, bioinspired total synthesis of dimeric piperine alkaloids in batch and flow

Mohammed Latrache, [a] Amina Sesay, [a] Samuel Oger, [a] Mireia Benito Montaner, [b] Jinlei Zhang, [c] Mohamed Mellah, [d] Erwan Poupon, [a] Stephen T. Hilton, [b] Stellios Arseniyadis [c] and Laurent Evanno *[a]

We report a unified, bioinspired synthesis of nigramide R, chabamide, and dipiperamides F and G *via* catalyst-controlled photocatalytic dimerization of piperine. Selective [2+2] and [4+2] cycloadditions in batch or flow provide access to diverse dimeric alkaloids from a common precursor. A low-cost, 3D-printed continuous-flow PhotoFlow reactor improves efficiency and reproducibility, establishing a modular strategy for these compounds.

The biosynthesis of complex natural products frequently relies on pericyclic reactions, particularly [2+2] and [4+2] cycloadditions, to generate architecturally intricate frameworks from simple precursors.[1,2] While such disconnections are intuitively appealing in retrosynthetic analysis, their direct implementation on fully functionalized substrates remains a formidable challenge. Photochemical cycloadditions conducted under conventional batch conditions often require prolonged irradiation, leading to substrate photodegradation and competing side reactions that compromise efficiency and selectivity. Continuous-flow photochemistry has emerged as a powerful solution to these intrinsic limitations. Compared to batch processes, flow systems offer enhanced mass and heat transfer, improved photon flux and light penetration, and precise control over reaction parameters, enabling faster and more reproducible transformations.[3] The small path lengths of flow reactors minimize dark zones and ensure uniform irradiation, which is especially advantageous for photocatalytic reactions. In addition, continuous processing facilitates scalability, safe handling of reactive intermediates, and integration into multi-step sequences with reduced purification steps and waste generation as demonstrated in several reported total syntheses.[4]

Recently, Hilton and co-workers reported a low-cost, fully 3D-printed continuous-flow platform operated by compressed air or nitrogen.[5–9] This modular, "plug-and-play" system integrates photochemical reactors with in-line sensing and enables precise control of flow rate, temperature, and irradiation intensity. Its affordability, operational simplicity, and reproducibility significantly lower the barrier to entry for flow photochemistry in academic laboratories. Building on these advantages, we sought to apply this technology to the synthesis of natural piperine dimers, which along with the aplysinopsin alkaloids,[10,11] have attracted our attention due to their structural complexity arising from [2+2] and [4+2] assemblies (Fig. 1). Piperine dimers, isolated from *Piper* species such as *P. nigrum* (black pepper), comprise a structurally diverse family featuring either vinylcyclobutane or cyclohexene cores. Members of this class, including the nigramides,

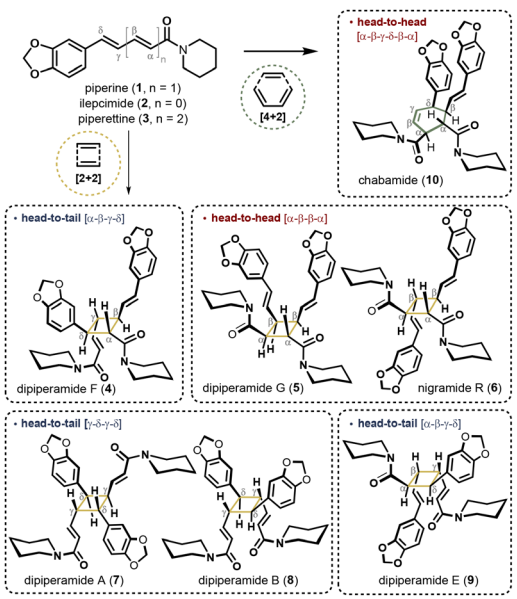

Fig. 1 Structure of natural piperine dimers from [2+2] or [4+2] assemblies.

[a] BioCIS, CNRS, Université Paris-Saclay, 91400 Orsay, France. E-mail: laurent.evanno@universite-paris-saclay.fr
[b] UCL School of Pharmacy, University College London, 29-39 Brunswick Square, WC1N 1AX, London, UK
[c] Queen Mary University of London, Department of Chemistry, Mile End Road, E1 4NS, London, UK
[d] ICMMO, CNRS, Université Paris-Saclay, 91400 Orsay, France

chabamides, and dipiperamides (**4**–**10**), are believed to arise from self-dimerization of piperine (**1**) or from cross-assemblies with related congeners such as ilepcimide (**2**) and piperettine (**3**).[12–20]

Despite their intriguing architectures, synthetic studies of these dimers remain limited. Key advances include direct [4+2] assemblies of piperine (**1**),[21,22] synthesis of the proposed cyclobutane structure of pipercyclobutanamide A,[13,23] preparation of related congeners *via* cinnamate dimerization strategies,[24,25] and Yoon's asymmetric [2+2] photocycloaddition of cinnamoyl imidazoles *en route* to (+)-nigramide R (**6**).[26] Nevertheless, a direct, catalyst-controlled dimerization of native piperine that selectively accesses both [2+2] and [4+2] frameworks has not been realized. Herein, we report a unified and selective photocatalytic dimerization of natural piperine, enabled by continuous-flow technology, providing efficient access to structurally complex piperine dimers and establishing a platform for the streamlined synthesis of these alkaloids.

Over the past two decades, many photocatalytic [2+2] and [4+2] cycloadditions have been reported,[2,27–29] mainly *via* radical-cation cycloadditions of styrenes,[30–34] radical-anion cyclizations of acrylates,[35,36] or energy transfer processes.[26,37–39] For this study we aimed to develop a general photocatalytic approach to natural products derived from piperine (**1**). Prior to implementing a continuous-flow protocol to enable rapid synthesis, we conducted an extensive screening of ruthenium- and iridium-based photocatalysts. Piperine (**1**), an abundant and readily available starting material, can be viewed as a polyfunctional diene (Fig. 2): the α,β-olefin is predisposed to radical-anion activation, whereas the γ,δ-olefin is capable of radical-cation formation.

Initial investigations focused on four ruthenium complexes, $Ru(bpy)_3Cl_2$, $Ru(bpm)_3Cl_2$, $Ru(phen)_3Cl_2$ and $Ru(bpz)_3(PF_6)_2$, under diverse conditions, including the presence of co-oxidants (methyl viologen dichloride, air, or 4,4′-di-*tert*-butylbiphenyl), a reductant (*i*Pr_2NEt), or an inert argon atmosphere. Control experiments performed in the absence of photocatalyst under light irradiation revealed that dimerization occurred exclusively in the solid state and required prolonged irradiation over several days. Under UV-*B*-enriched white light, multiple dimeric products were formed, indicating poor selectivity. Irradiation with blue LEDs provided dipiperamide F (**4**), albeit in modest yield (22%). In contrast, all ruthenium catalysts evaluated in the presence of an oxidant resulted in either minimal conversion or substantial substrate degradation (see SI for full details, Table S1). Productive reactivity was observed using $Ru(bpy)_3Cl_2$ as catalyst in the presence of *i*Pr_2NEt (Table 1, entries 1 and 2). Under these conditions, the [2+2] cycloadducts dipiperamide F (**4**), dipiperamide G (**5**), and nigramide R (**6**) were obtained in 7%, 26%, and 45% isolated yield, respectively. The enhanced reactivity observed under reductive conditions initially suggested a single-electron reduction of the α,β-olefin *via* a reductive quenching pathway, generating a radical-anion intermediate. However, electrochemical studies prompted a complete reassessment of this mechanistic hypothesis (see next page for details).

The [2+2] cycloaddition between two piperine (**1**) units across their α,β-double bonds preferentially affords the head-to-head cycloadduct nigramide R (**6**). Dipiperamide G (**5**) arises from an analogous regioselective pathway but involves prior photoinduced *E*/*Z* isomerization of one piperine unit, consistent with the rapid formation of *E*/*Z* isomers observed during irradiation. The head-to-tail cycloadduct dipiperamide F (**4**) likely originates from a minor pathway involving addition of the α,β-olefin of one piperine molecule to the γ,δ-olefin of another. Comparable outcomes were obtained in DMSO and DMF (Table 1, entries 3 and 4). Interestingly, when $Ru(phen)_3Cl_2$ was employed under an inert argon atmosphere without an external electron donor (Table 1, entry 7), the same set of [2+2] cycloadducts was formed in comparable yields (**4** : 8%; **5** : 12%;**6** : 34%), albeit after seven days irradiation. To improve the [2+2] process, we evaluated the effect of $LiBF_4$ in combination with $Ru(bpy)_3Cl_2$ (Table 1, entries 5 and 6) as previously reported by Yoon.[36] After 16 h, the [4+2] cycloadduct chabamide (**10**) was isolated in 15% yield, together with the [2+2] cycloadducts, dipiperamide F (**4**, 17%) and nigramide R (**6**, 15%), alongside led to increased degradation; however, while the yield of dipiperamide F (**4**) remained unchanged (17%), chabamide (**10**) was obtained as the major product in 33% yield. A control experiment where a pure sample of nigramide R (**6**) was stirred for 16 h under blue LED irradiation in the presence of $LiBF_4$ showed no conversion to chabamide (**10**). After 40 h, chabamide (**10**) is ultimately isolated as the major product. This outcome appears to result from the need for extended irradiation times to fully consume the starting material combined with the lower propensity of **10** to undergo degradation compared to the [2+2] cycloadducts **5** and **6**, rather than from a reversible interconversion between products. The same approach was extended to a series of iridium photocatalysts, which included, *fac*-$Ir(ppy)_3$, $[Ir(dtbbpy)(ppy)_2]PF_6$, $[Ir(dFCF_3ppy)_2(bpy)]PF_6$ and $[Ir(dFCF_3ppy)_2(5,5'\text{-}dCF_3bpy)]PF_6$. Again, in the presence of an oxidant, such as methyl viologen dichloride, air or 4,4′-di-*tert*-butylbiphenyl, poor conversions of the starting material were observed independently of the catalyst used. The use of *fac*-$Ir(ppy)_3$ in the presence of *i*Pr_2NEt gave full conversion to the [4+2] cycloadducts **11** and **12** in 53% and 12% yield respectively (Table 1, entry 10),

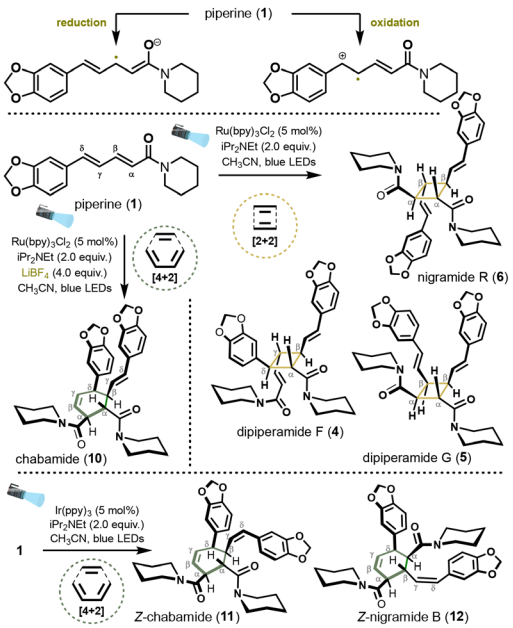

Fig. 2 Dimerization of piperine (**1**) by photocatalysis.

Table 1 Condition for the [2+2] or [4+2] cycloadditions of piperine (**1**)

Entry	Catalyst (5 mol%)	Conditions	Result[a]
1	$Ru(bpy)_3Cl_2$	CH_3CN, Ar atm. blue LEDs, 16 h	Low conversion <10%
2	$Ru(bpy)_3Cl_2$	CH_3CN, iPr_2NEt (2.0 equiv.) blue LEDs, 16 h	**1**: 10%; **4**: 7% **5**: 26%; **6**: 45%
3	$Ru(bpy)_3Cl_2$	DMSO, iPr_2NEt (2.0 equiv.) blue LEDs, 16 h	**1**: 6%; **4**: 9% **5**: 15%; **6**: 31%
4	$Ru(bpy)_3Cl_2$	DMF, iPr_2NEt (2.0 equiv.) blue LEDs, 16 h	**1**: 11%; **4**: 10% **5**: 33%; **6**: 38%
5	$Ru(bpy)_3Cl_2$	CH_3CN, iPr_2NEt (2.0 equiv.) $LiBF_4$ (4 equiv.), blue LEDs 16 h	**4**: 17%; **6**: 15% **10**: 15%
6	$Ru(bpy)_3Cl_2$	CH_3CN, iPr_2NEt (2.0 equiv.) $LiBF_4$ (4.0 equiv.) blue LEDs, 40 h	**4**: 17%; **10**: 33%
7	$Ru(phen)_3Cl_2$	CH_3CN, Ar atm. blue LEDs, 7 d	**4**: 8%; **5**: 12% **6**: 34%
8	$Ru(phen)_3Cl_2$	CH_3CN, iPr_2NEt (2.0 equiv.) blue LEDs, 40 h	<5% conversion
9	$Ru(phen)_3Cl_2$	CH_3CN, air atm. blue LEDs, 40 h	<5% conversion
10	*fac*-Ir(ppy)$_3$	CH_3CN, iPr_2NEt (2.0 equiv.) blue LEDs, 16 h	**11**: 53% **12**: 12%

[a] Isolated yields.

while all the other catalysts gave no or poor conversions (see Table S1 in the SI for full details). Both products **11** and **12** correspond to the *Z* isomers of chabamide (**10**) and nigramide B. To understand when isomerization occurred, compound **10** was irradiated under blue LEDs light in the presence of *fac*-Ir(ppy)$_3$ with and without iPr_2NEt. Interestingly, chabamide was recovered unchanged, suggesting that the *E*/*Z* isomerization of the γ,δ double occurs during the [4+2] assembly process rather than once the cycloadduct is formed. Just like with $Ru(bpy)_3Cl_2$, changing the base or the solvent did not significantly affect the outcome.

Regarding the dimerization mechanism of piperine (**1**), we initially hypothesized reductive quenching cycles, as the use of iPr_2NEt was found to accelerate the reactions and facilitate their completion. The electrochemical behaviour of substrates **1**, was evaluated by cyclic voltammetry in acetonitrile (see SI for full details). Substrate **1** exhibits an irreversible oxidation wave with the first peak potential at +1.35 V *vs.* SCE, followed by two additional oxidation events at +1.75 V and +1.98 V. On the reductive side, **1** exhibits a well-defined irreversible reduction wave (E_{red} = −1.88 V). Based on these potentials, a reductive quenching cycle is thermodynamically conceivable when *fac*-Ir(ppy)$_3$ ($E_P/_{P^-}$ = −2.19 V) is used in the presence of iPr_2NEt as single-electron reduction of **1** is energetically accessible. In contrast, the excited-state reduction potential of $Ru(bpy)_3Cl_2$ ($E_P/_{P^-}$ = −1.33 V) is insufficient to reduce **1**, rendering a reductive quenching pathway unlikely under these conditions and instead supporting an energy-transfer mechanism. Consistent with this interpretation, reactions conducted in the absence of iPr_2NEt showed low conversion (Table 1, entry 1), whereas addition of the amine led to complete consumption of the starting material. We therefore propose that in the $Ru(bpy)_3Cl_2$ system, iPr_2NEt does not function as an electron donor but rather modulates the reaction environment, potentially through substrate association or deprotonation, thereby facilitating productive energy transfer.

Following the identification of the most effective photocatalytic systems, several intrinsic limitations of the batch protocol became apparent. Both [2+2] and [4+2] dimerizations proceeded with only moderate conversions and required prolonged irradiation (*ca.* 16 h) to achieve synthetically useful yields. These extended exposure times also increased the extent of product degradation. To address these challenges, we translated the optimized conditions to a modular, 3D-printed continuous-flow platform (Fig. 3). This transition was motivated by two primary objectives: (i) reduction of reaction times through improved and more uniform photon flux, and (ii) enhancement of yields by minimizing photodegradation associated with extended irradiation. The setup comprises modular reactor blocks connected in series, enabling precise control over residence time and irradiation parameters. The setup

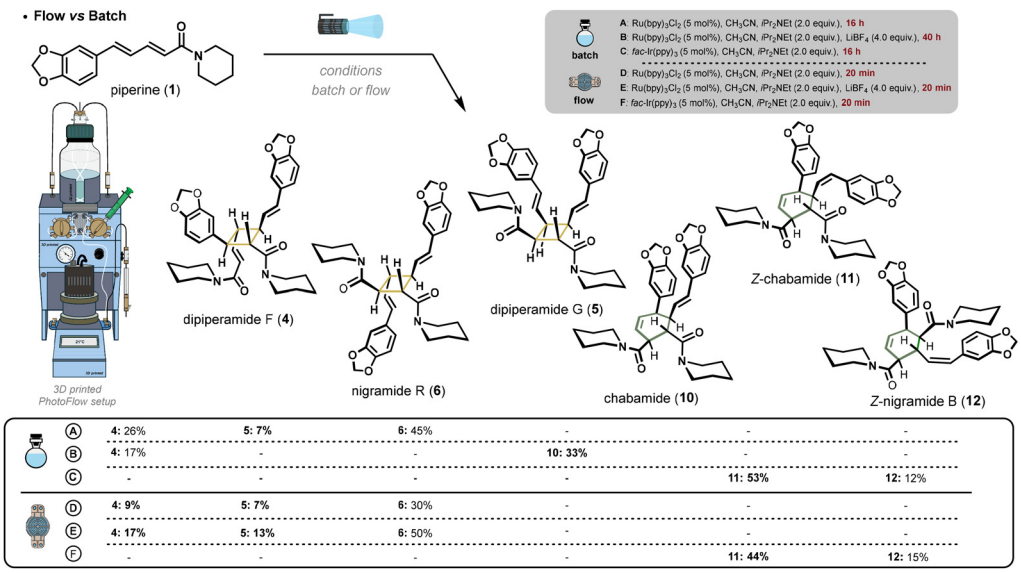

Fig. 3 Batch *vs.* flow synthesis of piperine dimers.

comprises modular reactor blocks connected in series. Nitrogen pressure drives the reaction solution through injection loops at typical flow rates of 0.1–1.0 mL min^{-1}, eliminating the need for mechanical pumps. The narrow channel dimensions ensure uniform light penetration, minimize dark zones, and provide high reproducibility. The reactor is air-cooled and irradiated with a 456 nm Kessil® lamp. Residence time is readily adjusted by varying the flow rate and by configuring the system to incorporate one or both reaction compartments in series. In our studies, a single injection loop containing a premixed solution of substrate and photocatalyst was employed, with both reactor compartments connected sequentially to maximize irradiation efficiency (See SI for full details). After minimal optimization, the dimerization of piperine (**1**) proceeded efficiently under flow conditions, requiring only a 20 min residence time at a flow rate of 0.1 mL min^{-1}, compared to 16 h under batch irradiation. Using $Ru(bpy)_3Cl_2$ (5 mol%) and iPr_2NEt (2.0 equiv.) in CH_3CN (0.12 M), a moderate conversion of 50% was observed by ^1H NMR spectroscopy. Notably, addition of $LiBF_4$ (4 equiv.), consistent with Yoon's observations,[35] markedly enhanced reaction efficiency and led to complete conversion. Under these conditions, dipiperamides F (**4**) and G (**5**), together with the kinetic product nigramide R (**6**), were isolated in 17%, 13%, and 50% yield, respectively. Compared to the batch process, the yield of nigramide R (**6**) was slightly improved. Moreover, the shorter irradiation time under the flow conditions significantly reduced the formation of dipiperamide G (**5**), which originates from photoinduced *E*/*Z* isomerization of piperine (**1**) prior to cycloaddition. Notably, the decreased residence time enabled exclusive formation of the [2+2] cycloadducts, with no detectable formation of the competing [4+2] product chabamide (**10**). Extending the PhotoFlow conditions [*fac*-$Ir(ppy)_3$ (5 mol%), iPr_2NEt (2.0 equiv.), CH_3CN (0.12 M), 0.1 mL min^{-1}, 20 min residence time] to the corresponding dimerization reactions furnished the targeted products **11** and **12** in 44% and 15% yield, respectively. Reducing the residence time to 10 min (0.2 mL min^{-1}) resulted in incomplete substrate conversion, with approximately 15% of unreacted **1** remaining in the crude reaction mixture. As a control experiment, reproducing the optimized conditions in batch for 20 min resulted in less than 5% conversion, further highlighting the significant enhancement in reaction kinetics under flow conditions

In summary, we demonstrate that catalyst-controlled photocycloaddition of piperine enables selective access to distinct cycloadduct frameworks through divergent reactivity. By modulating the photocatalytic system, regioselective [2+2] and [4+2] cycloadditions can be achieved, allowing the synthesis of nigramide R, chabamide, dipiperamide F and G, or their respective isomers depending on the catalytic system used. The method was also applied to the triene congener piperettine (**3**), enabling the formation of the head-to-head [4+2] cycloadduct (not shown, see SI for full details). Implementation of continuous-flow photochemistry using a standardized, modular, 3D-printed PhotoFlow platform markedly reduced reaction times from days to minutes, thereby minimizing substrate isomerization prior to cycloaddition and enhancing diastereoselectivity. Collectively, this work establishes a general and operationally practical strategy for the synthesis of structurally complex dimeric natural product architectures.

Conflicts of interest

There are no conflicts to declare.

Data availability

All data supporting this study are provided in the supplementary information (SI). Supplementary information: experimental procedures, full screening results, the synthesis of piperettine and its [4+2] photocatalyzed dimerization, compound characterisation, electrochemical measurements, and NMR spectra. See DOI: https://doi.org/10.1039/d6cc01304j.

Acknowledgements

We thank the Agence Nationale de la Recherche (SMASH, ANR-2020-CE07-0021-01), Université Paris-Saclay, the CNRS, Queen Mary University of London and University College London for financial support and facilities. The authors thank Rémi Franco and Jean-Christophe Jullian for NMR assistance, and Karine Leblanc and Somia Rharrabti for LC-HRMS analyses.

References

1 K. C. Nicolaou, S. A. Snyder, T. Montagnon and G. Vassilikogiannakis, *Angew. Chem., Int. Ed.*, 2002, **41**, 1668–1698.
2 D. Sarkar, N. Bera and S. Ghosh, *Eur. J. Org. Chem.*, 2020, 1310–1326.
3 L. Capaldo, Z. Wen and T. Noël, *Chem. Sci.*, 2023, **14**, 4230–4247.
4 L. Wan, G. Kong, M. Liu, M. Jiang, D. Cheng and F. Chen, *Green Synth. Catal.*, 2022, **3**, 243–258.
5 M. R. Penny and S. T. Hilton, *J. Flow Chem.*, 2023, **13**, 435–442.
6 M. R. Penny, Z. X. Rao, B. F. Peniche and S. T. Hilton, *Eur. J. Org. Chem.*, 2019, 3783–3787.
7 M. B. Montaner and S. T. Hilton, *Curr. Opin. Green Sustainable Chem.*, 2024, **47**, 100923.
8 J. Zhang, E. Selmi-Higashi, S. Zhang, A. Jean, S. T. Hilton, X. C. Cambeiro and S. Arseniyadis, *Org. Lett.*, 2024, **26**, 2877–2882.
9 A. Hannam, P. Kankraisri, K. R. Thombare, P. Meher, A. Jean, S. T. Hilton, S. Murarka and S. Arseniyadis, *Chem. Commun.*, 2024, **60**, 7938–7941.
10 S. Oger, N. Duchemin, Y. M. Bendiab, N. Birlirakis, A. Skiredj, S. Rharrabti, J.-C. Jullian, E. Poupon, M. Smietana, S. Arseniyadis and L. Evanno, *Chem. Commun.*, 2023, **59**, 4221–4224.
11 N. Duchemin, A. Skiredj, J. Mansot, K. Leblanc, J.-J. Vasseur, M. A. Beniddir, L. Evanno, E. Poupon, M. Smietana and S. Arseniyadis, *Angew. Chem., Int. Ed.*, 2018, **57**, 11786–11791.
12 Y. Fujiwara, K. Naithou, T. Miyazaki, K. Hashimoto, K. Mori and Y. Yamamoto, *Tetrahedron Lett.*, 2001, **42**, 2497–2499.
13 R. Liu, M. Zhang, T. P. Wyche, G. N. Winston-McPherson, T. S. Bugni and W. Tang, *Angew. Chem., Int. Ed.*, 2012, **51**, 7503–7506.
14 C. E. Mair, R. Liu, A. G. Atanasov, L. Wimmer, D. Nemetz-Fiedler, N. Sider, E. H. Heiss, M. D. Mihovilovic, V. M. Dirsch and J. M. Rollinger, *Planta Med.*, 2015, **81**, 1065–1074.
15 S. Tsukamoto, B.-C. Cha and T. Ohta, *Tetrahedron*, 2002, **58**, 1667–1671.
16 R. Muharini, Z. Liu, W. Lin and P. Proksch, *Tetrahedron Lett.*, 2015, **56**, 2521–2525.
17 K. Wei, W. Li, K. Koike, Y. Chen and T. Nikaido, *J. Org. Chem.*, 2005, **70**, 1164–1176.
18 V. R. S. Rao, G. Suresh Kumar, V. U. M. Sarma, S. Satyanarayana Raju, K. Hari Babu, K. Suresh Babu, T. Hari Babu, K. Rekha and J. M. Rao, *Tetrahedron Lett.*, 2009, **50**, 2774–2777.
19 V. Gómez-Calvario and M. Y. Rios, *Magn. Reson. Chem.*, 2019, **57**, 994–1070.
20 H. Matsuda, K. Ninomiya, T. Morikawa, D. Yasuda, I. Yamaguchi and M. Yoshikawa, *Bioorg. Med. Chem.*, 2009, **17**, 7313–7323.
21 K. Wei, W. Li, K. Koike and T. Nikaido, *Org. Lett.*, 2005, **7**, 2833–2835.

22 V. R. S. Rao, G. Suresh, K. S. Babu, S. S. Raju, M. V. P. S. Vishnuvardhan, S. Ramakrishna and J. M. Rao, *Tetrahedron*, 2011, **67**, 1885–1892.
23 W. R. Gutekunst, R. Gianatassio and P. S. Baran, *Angew. Chem., Int. Ed.*, 2012, **51**, 7507–7510.
24 M. Takahashi, M. Ichikawa, S. Aoyagi and C. Kibayashi, *Tetrahedron Lett.*, 2005, **46**, 57–59.
25 I. Colomer, R. Coura Barcelos and T. J. Donohoe, *Angew. Chem., Int. Ed.*, 2016, **55**, 4748–4752.
26 M. J. Genzink, M. D. Rossler, H. Recendiz and T. P. Yoon, *J. Am. Chem. Soc.*, 2023, **145**, 19182–19188.
27 T. P. Yoon, *ACS Catal.*, 2013, **3**, 895–902.
28 C. K. Prier, D. A. Rankic and D. W. C. MacMillan, *Chem. Rev.*, 2013, **113**, 5322–5363.
29 D. A. Nicewicz and T. M. Nguyen, *ACS Catal.*, 2014, **4**, 355–360.
30 S. Lin, M. A. Ischay, C. G. Fry and T. P. Yoon, *J. Am. Chem. Soc.*, 2011, **133**, 19350–19353.
31 S. M. Stevenson, R. F. Higgins, M. P. Shores and E. M. Ferreira, *Chem. Sci.*, 2016, **8**, 654–660.
32 S. Lin, C. E. Padilla, M. A. Ischay and T. P. Yoon, *Tetrahedron Lett.*, 2012, **53**, 3073–3076.
33 K. Nakayama, N. Maeta, G. Horiguchi, H. Kamiya and Y. Okada, *Org. Lett.*, 2019, **21**, 2246–2250.
34 M. Riener and D. A. Nicewicz, *Chem. Sci.*, 2013, **4**, 2625–2629.
35 M. A. Ischay, M. E. Anzovino, J. Du and T. P. Yoon, *J. Am. Chem. Soc.*, 2008, **130**, 12886–12887.
36 J. Du and T. P. Yoon, *J. Am. Chem. Soc.*, 2009, **131**, 14604–14605.
37 E. M. Sherbrook, H. Jung, D. Cho, M.-H. Baik and T. P. Yoon, *Chem. Sci.*, 2020, **11**, 856–861.
38 E. M. Sherbrook, M. J. Genzink, B. Park, I. A. Guzei, M.-H. Baik and T. P. Yoon, *Nat. Commun.*, 2021, **12**, 5735.
39 L.-M. Zhao, T. Lei, R.-Z. Liao, H. Xiao, B. Chen, V. Ramamurthy, C.-H. Tung and L.-Z. Wu, *J. Org. Chem.*, 2019, **84**, 9257–9269.